AIAA 99-3806

Vortex Dynamics in the Sphere Wake

R. Mittal‡
Department of Mechanical Engineering
University of Florida
Gainesville, Florida, 32611
F.M. Najjar†
Center for Simulation of Advanced Rockets
University of Illinois at Urbana-Champaign
Urbana, Illinois 61801

ABSTRACT

A highly accurate Fourier-Chebyshev spectral collocation method has been used to simulate flow in the wake of a sphere in the Reynolds number range from 350 to 650. Flow visualizations and frequency spectra provide a glimpse of the complex vortex dynamics that are observed in the sphere wake. It is found that in addition to the vortex shedding frequency which corresponds to the shedding of large-scale vortex loops in the wake other lower and higher frequencies are also present and the complex evolution of the vortices in the wake is a result of the non-linear interaction of these frequencies. The response of the sphere wake to flow perturbations is also addressed. Interestingly, it is found that the sphere wake exhibits classic symptoms of the vortex shedding "lock-on" phenomenon which has hitherto been observed mainly in 2-D bluff-body wakes.

1. INTRODUCTION

The sphere wake which is a prototypical axisymmetric wake is not as well understood as its two-dimensional counter part, the circular cylinder wake. Studies to date indicate that vortex shedding in the sphere wake is substantially different from that in the wake of a cylinder and therefore little of what has been learnt for 2-D bluff body wakes is directly applicable to axisymmetric wakes. Detailed investigation of the structure of the sphere wake were initiated by Margavey and co-workers[9,10] who mapped out the various transition ranges in the sphere wake over a range of Reynolds numbers. More recent experiments[17,19,18] and numerical simulations[8,11,12,16,20] have also added to our knowledge of the various bifurcations that the sphere wake undergoes as the Reynolds number is increased. Based on these studies it is known that vortex shedding in the sphere wake occurs for Reynolds numbers greater than about 300. As the Reynolds number is increased beyond this value the vortex shedding process goes through a series of bifurcations which successively increase its complexity. Although a number of previous investigations have reported these bifurcations very little consensus exists regarding the nature of these bifurcations.

From the point of view of flow-structure interaction it is also of interest to understand how the sphere wake behaves when exposed to a perturbed flow. Cylinder wakes exhibit the phenomenon of vortex shedding "lock-on" where the vortex shedding can lock-on to a forcing frequency which is different from the natural shedding frequency[1,3,5,6,7,15]. One characteristic feature of vortex shedding from cylinders is that every shedding cycle involves the formation of two counter-rotating vortices. As a result of this, the lift oscillates at the shedding frequency whereas the drag oscillates at twice the shedding frequency. Thus the cylinder wake exhibits a strong superharmonic component. In contrast vortex shedding from a sphere at low Reynolds numbers involves the formation of one vortex loop per shedding cycle and thus a significant superharmonic component does not exist[12]. This difference between the two wakes is expected to result in a markedly different response to flow perturbations.

In the current study we therefore address two aspects of vortex shedding in sphere wakes (1) The complexity of the vortex dynamics observed in the sphere wake in the transitional range $350<\mathrm{Re}_d<650$ (2) The response of the sphere wake to freestream perturbations and vortex shedding lock-on in a sphere wake.

2. NUMERICAL METHODOLOGY

A solver based on a Fourier–Chebyshev spectral collocation has been developed for direct numerical simulation of three-dimensional, viscous, incompressible flow past a prolate spheroid. Flow past a sphere can be solved as a special case. Here we present only a brief outline of the solver used for the current simulations. For a detailed description the reader is referred to Mittal[11] .

The governing equations are the unsteady, incompressible Navier-Stokes equations given by

$$\nabla . \boldsymbol{u} = 0 \tag{1}$$

$$\frac{\partial \boldsymbol{u}}{\partial t} + \boldsymbol{u}.\nabla \boldsymbol{u} = -\nabla P + \frac{1}{\mathrm{Re}_d}\nabla^2 \boldsymbol{u} \tag{2}$$

where $\boldsymbol{u}$ and P are the velocity and pressure respectively and Re_d is the Reynolds number based on the freestream velocity (U_∞) and diameter (d) of the sphere. The above equations are transformed to the prolate spheroidal coordinate system and

‡Assistant Professor, Member
†Research Scientist, Member

discretized on an orthogonal curvilinear body-fitted grid. The azimuthal direction ϕ is periodic over 2π and this allows us to use a Fourier collocation method in this direction. In the θ–direction, which is referred to as the wall-tangential direction, the flow is periodic not over π but over 2π, and a restricted Fourier series is used for computing derivatives along this direction. The algorithm also allows us to cluster more points in the wake in the θ–direction. The semi-infinite flow domain is truncated to a large but finite distance and a Chebyshev collocation method is used in this non-periodic direction. Thus, spectral discretization is used in all the three directions resulting in a highly accurate computation of the spatial derivatives.

A two-step time-split scheme[4] is used for advancing the solution in time. The intermediate velocity field is obtained first by advancing through the advection-diffusion equation. and a second-order accurate, semi-implicit method is used for this step. The radial and azimuthal viscous terms are discretized in an implicit manner using a Crank-Nicolson scheme. All other terms such as the non-linear convection and other cross-terms that result from the curvilinear nature of the coordinate system are treated explicitly using a 2nd-order Adams-Bashforth scheme. The next step is pressure-correction and this requires the solution of the pressure Poisson equation which is solved with a homogeneous Neumann condition on the boundaries. Finally the pressure correction is added to the intermediate velocity and a divergence-free velocity field is obtained. A higher order boundary condition for the intermediate velocity is used which results in accurate imposition of the no-slip, no-penetration condition on the body. Details of the time-split scheme can be found in Mittal[11]. Figure 1 shows a 2-D cut of a typical grid used in our simulations. The 3-D mesh is obtained by a rotation of the 2-D mesh about the axis of the sphere.

Since the flow domain is truncated to a finite extent in the current simulations, appropriate boundary conditions are required at the outer boundary. Inviscid flow past the spheroid is computed first and this is used as the inflow boundary condition as well as the initial condition. At the outflow boundary we use a previously developed non-reflective boundary condition which allows vortical disturbances to exit the computational domain in a smooth manner without any significant reflections. This boundary treatment has been tested extensively in cylindrical and spheroidal geometries and details of these tests can be found in Mittal & Balachandar[14] and Mittal[11].

3. RESULTS AND DISCUSSIONS

Natural Vortex Shedding

The current study will focus on the $350<Re_d<650$ regime. It is known from previous studies[16,18] that for Reynolds numbers lower than 300 small scale perturbations do not lead to vortex shedding in the wake. However at higher Reynolds number, perturbation are amplified by the inherent instability of the wake and leads to a dynamically complex vortex shedding process. In the current simulations a small perturbation is given for a short duration of time at the beginning and the flow is then allowed to develop naturally. The perturbation grows under the influence of the inherent wake instability and results in vortex shedding. Each simulation is integrated in time until a stationary state is obtained and this can take up to $200d/U_\infty$. The simulation is run over an additional time interval of about $120d/U_\infty$ after the stationary state is reached.

Figure 2a shows the vortex topology in the wake of the sphere at Re_d=350. The vortices in the wake have been identified by plotting one isosurface of the imaginary part of the eigenvalue of the velocity gradient tensor. The most striking feature observed in the bottom view of Figure 2a is the apparent symmetry of the wake about a plane passing through the wake centerline. This peculiar condition has been the subject of a previous paper[12] where it has been shown that this planar symmetric vortex shedding may exist upto a Reynolds number of about 375. Figure 3a shows the frequency spectra corresponding to the temporal variation of the transverse velocity component at one location in the near wake. The spectra indicates a vortex shedding Strouhal number of 0.138 ± 0.003. However, in addition to the vortex shedding frequency, the spectra also shows a peak at 0.040 ± 0.003. The dotted line shows the spectra from the computation of Bagchi & Balachandar[2] which employs a different solver. The power spectral density of their plot has been scaled down in order to fit both curves on the same plot. Their simulation predicts a vortex shedding frequency of 0.135 ± 0.005 and a lower frequency of 0.034 ± 0.005 both of which are in good agreement with our simulation.

Figure 2b and c show the vortex topology for Re_d=500 and 650 respectively. In both cases it can be seen that the orientation of the vortex varies significantly from cycle to cycle. Furthermore, both figures shows the formation of vortex rings in the downstream region of the wake and this is in line with the observations of Margavey & Bishop[9]. Figure 3b shows the spectra for the Re_d=500 case and we find that the shedding frequency for this case is 0.150 ± 0.006†. However in addition to the vortex shedding frequency, lower frequencies of 0.05 and 0.025 also exist. A similar low frequency has also been observed in the simulation of Tomboulides et al.[20] Figure 3c shows the frequency spectra for Re_d=650 and we find that the vortex shedding Strouhal number is 0.176 ± 0.008. In addition to this the spectra also clearly shows a peak at a higher frequency of 0.272 ± 0.008. Thus, even though there does not seem to be a significant difference in the topology of the wake at these two Reynolds number, the spectra indicates that the dynamics of the wake are quite different.

The presence of the high frequency in the Re_d=650 is somewhat surprising. As shown in Figure 4, experiments[19] indicate a "high-mode" of shedding in the wake at Reynolds numbers higher than about 800. This shedding mode is associated with the formation of shear layer vortices in the separated shear layers which typically occurs at a frequency

†In Mittal[11] this frequency was erroneously given to be 0.186.

higher than the vortex shedding frequency. Our simulation show the presence of a higher frequency at a Reynolds number of 650 which would indicate that the onset of the high-mode occurs at a lower Reynolds number than previously reported. However, this is not confirmed by flow visualizations. Figure 5 shows a contour plot of the instantaneous azimuthal vorticity distribution and no rollup of the separating shear layers can be observed. It is possible that the higher frequency is created due to non-linear interaction between the vortex shedding frequency and other lower frequencies but further analysis is needed in order to confirm this hypothesis.

Vortex Shedding Lock-On in Perturbed Flow

Previous studies[1,3,5,6,7,15] of flow past circular cylinders have shown that in the presence of an external periodic forcing mechanism, vortex shedding from a cylinder can lock-on to frequency of the external forcing. The forcing can either come from free/forced vibrations of the cylinder or from perturbations in the surrounding flow. This phenomenon has importance in flow-structure interaction since for an elastically mounted cylinder lock-on is usually accompanied by large amplitude vibration. Furthermore, this phenomenon suggests a means for active control of vortex shedding from bluff-body wakes.

Flow induced vibrations of spherical bodies is also of relevance to marine systems (towed arrays, underwater mines, UUVs). However, even though extensive work has been done on studying the lock-on phenomenon in cylinder wakes, very scant information exists regarding similar behavior in sphere wakes. In the current study we have performed a series of simulations in order to shed some light on the nature of vortex-shedding lock-on in sphere wakes. In these simulations a sinusoidal perturbation is applied to the cross-flow (u_y) velocity component. Thus the flow velocity prescribed at the inflow of the computational domain which is located $15d$ upstream of the sphere is given by:

$$\begin{Bmatrix} u_x \\ u_y \\ u_z \end{Bmatrix} = \begin{Bmatrix} 1 \\ A_{in}\sin(2\pi\Omega_e t) \\ 0 \end{Bmatrix} \qquad (3)$$

where A_{in} is the amplitude and Ω_e the nondimensional frequency ($\Omega_e = Fd/U_\infty$ where F is the fluctuation frequency) of the perturbation. The inlet perturbation decays at it convects into the domain due to viscous action and this decay depends strongly on the perturbation frequency. In the current simulations, A_{in} is chosen for each perturbation frequency so as to produce a 2% fluctuation at a location $5d$ upstream of the sphere. This ensures that the fluctuation level experienced by the sphere is for the most part independent of the perturbation frequency. Further details regarding the procedure for imposing the perturbation can be found in Mittal[13].

A series of simulation have been carried out where the perturbation frequency has been varied over the range $0.05 \le \Omega_e \le 0.3$. Here we present results of three simulations each of which demonstrate distinct behaviors of the forced wake. Figure 6a shows the frequency spectra obtained from the temporal variation of the transverse velocity at one location in the near wake ($x/d \approx 4$) for the case where Ω_e=0.3. The location is chosen to be the same as Figure 3a so that a direct comparison can be made. No significant peak is observed at the forcing frequency indicating that the vortex shedding does not respond to this forcing frequency. Figure 6b shows the corresponding power spectra for the Ω_e=0.2 simulation and this spectra clearly shows a peak at the forcing frequency in addition to a comparable peak at the natural shedding frequency. This type of spectra is indicative of vortex shedding lock-on.

Finally, Figure 6c shows the frequency spectra for the case of Ω_e=0.15 which is roughly 9% higher than the shedding frequency. The spectra indicates the absence of the natural shedding frequency. Instead the vortex shedding now occurs exclusively at the forcing frequency and this is termed as "complete lock-on." In our simulations complete lock-on is also observed for a forcing frequency of 0.10 which is about 27% lower than the shedding frequency. Thus, even at this low level of freestream perturbation, the sphere wake exhibits a rather large lock-on frequency range. Our previous simulations[13] have shown that the vortex shedding process in the sphere wake is considerably weaker than that in the cylinder wake. Although direct comparisons of the vortex strengths between the two flows have not been made, the lower fluctuation level of lift (or side) force and lower fluctuation intensities in the the sphere wake provide indirect proof for this assertion. It therefore follows that the sphere wake will be susceptible to perturbations of a lower amplitude than the cylinder wake.

4. CONCLUSIONS

Direct numerical simulations of the sphere wake have been performed to gain some insight into the complexity of the vortex shedding process in the range $350<\mathrm{Re}_d<650$. It has been found that the sphere wake at these transitional Reynolds numbers exhibits multiple dominant frequencies and the non-linear interaction between these frequencies leads to a complex evolution of vortex structures in the near wake. The physical mechanisms associated with the frequencies other than the vortex shedding frequency are not clear at this point and are the subject of an ongoing study. Simulations of flow past a sphere in a flow with transverse velocity perturbations show that the sphere-wake is susceptible to the classic lock-on phenomenon which to date been reported only in cylinder wakes.

ACKNOWLEDGEMENTS

These simulations have been performed on the SGI Origin-2000 at NCSA.

REFERENCES

1 Barbi, C., Favier, D.P., Maresca, C.A. and Telionis, D.P. 1986, Vortex Shedding and Lock-On of a Circular Cylinder in Oscillatory Flow. *J. Fluid Mech.*, Vol. 170, 527-544.

2 Bagchi, P. and Balachandar S. 1999, *Private Communication*.

3 Bearman, P.W. 1984 Vortex Shedding from Oscillating Bluff Bodies. *Ann. Rev. Fluid. Mech.*, 16, 195-222.

4 Chorin, A.J., 1968, "Numerical Solution of the Navier-Stokes Equations," *Math. Comput.*, 22, 745-757.

5 Griffin, O.M. and Hall, M.S. 1991 Review-Vortex Shedding Lock-on and Flow Control in Bluff-Body Wakes. *J. Fluids Engr.* Vol 113, 526-537.

6 Griffin, O.M. and Ramberg, S.E. 1974 The Vortex Street Wakes of Vibrating Cylinders. *J. Fluid Mech,* Vol. 66, 553-576.

7 Hall, M.S. and Griffin, O.M. 1993 Vortex Shedding and Lock-On in a Perturbed Flow. *J. Fluids Engr.* Vol 115, 283-291.

8 Johnson, T.A. and Patel, V.C. 1999. Flow Past a Sphere up to a Reynold Number of 300. *J. Fluid Mech.* Vol. 378, 19-70.

9 Margavey, R.H. and Bishop, R.L. 1961, "Transition Ranges for Three-Dimensional Wakes," *Can. J. Phys*. 39, 1418-1422.

10 Margavey, R.H. and MacLatchy, C.S. 1965, "Vortices in Sphere Wakes," *Can. J. Phys.* 43, 1649-1656.

11 Mittal, R. 1999 A Fourier Chebyshev Spectral Collocation Method for Simulating Flow Past Spheres and Spheroids. To appear in *Int. J. Numer. Meths. Fluid*s.

12 Mittal, R. 1999 Planar Symmetry in the Unsteady Wake of a Sphere. *AIAA J.* Vol. 37, No. 3, 388-391.

13 Mittal, R. 1999 Response of the Sphere Wake to Freestream Fluctuations. Submitted to *Phys. Fluids.*

14 Mittal, R. and Balachandar, S., 1996 "Direct Numerical Simulation of Flow Past Elliptic Cylinders," *J. Comp. Phys.,* 124, 351-367.

15 Moretti P.M. 1995 Fluid-Elastic Excitation in Heat Exchanger Tube Bundles. *EPRI TR-103507*.

16 Natarajan, R. and Acrivos, A. 1993, "The Instability of the Steady Flow Past Spheres and Disks," *J. Fluid Mech.*, 254, 323-344.

17 Ormieres, D. and Provensal, M. 1998. "Transition ot Turbulence in the Wake of a Sphere," Submitted to *Phys. Rev. Lett.*

18 Sakamoto H. and Haniu, H. 1990, "A Study of Vortex Shedding From Spheres in a Uniform Flow," *J. Fluids Engr.*, 112, 386-392.

19 Sakamoto, H. and Haniu, H. 1995 "The Formation Mechanism and Shedding Frequency of Vortices from a Sphere in Uniform Shear Flow" *J. Fluid Mech.*, 287, 151-171.

20 Tomboulides, A.G., Orszag, S.A. and Karniadakis, G.E., 1993, "Direct and Large-Eddy Simulations of Axisymmetric Wakes," *AIAA-93-0546*.

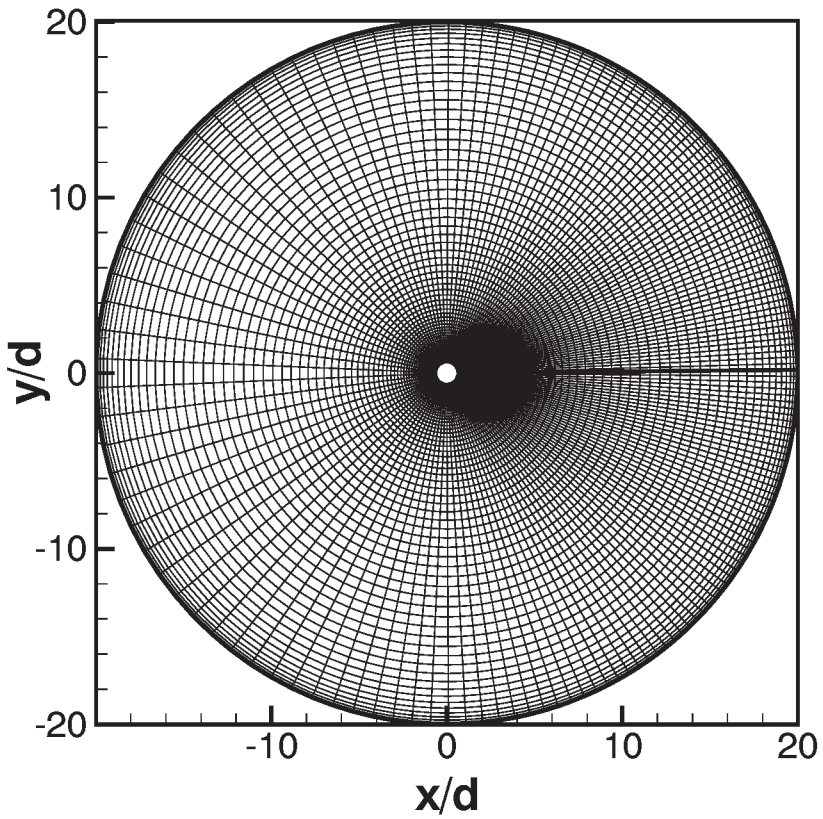

Figure 1. Grid used in the current simulations

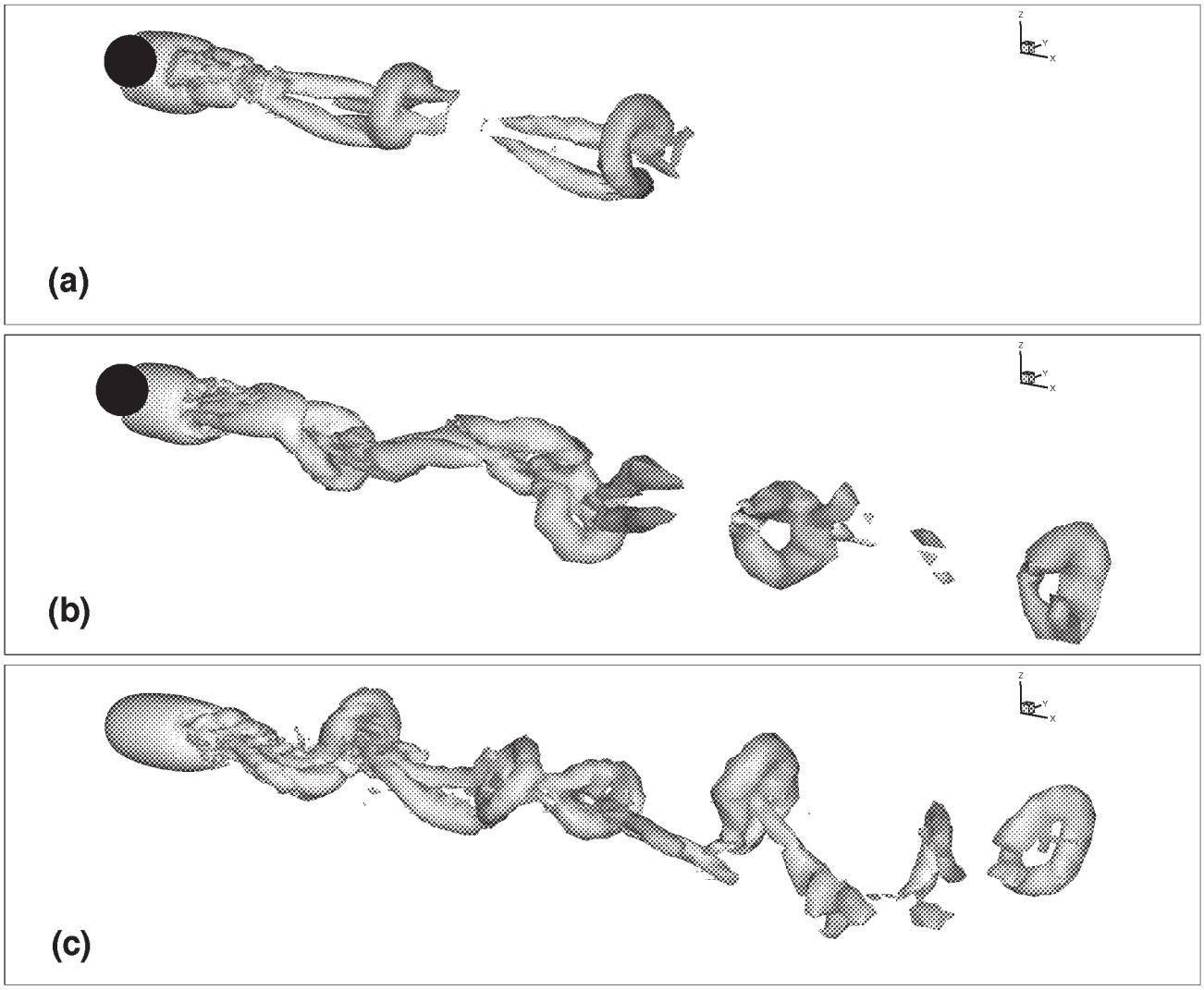

Figure 2. Vortex structures in the sphere wake (a) Re_d=350 (b) Re_d=500 (c) Re_d=650.

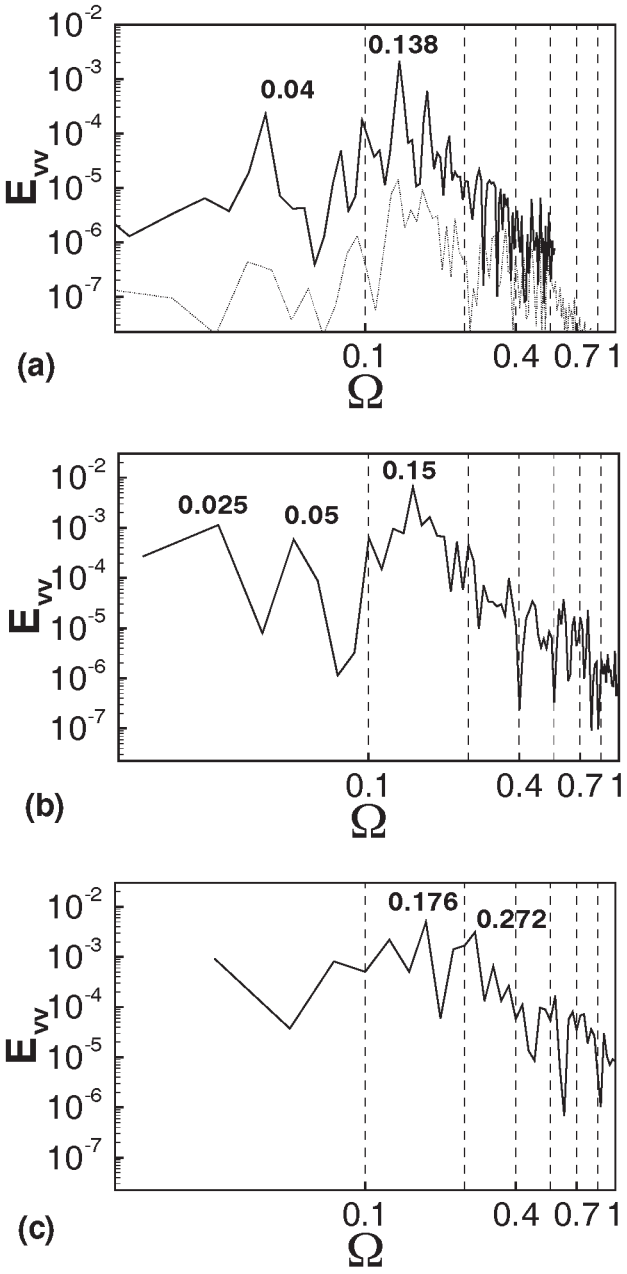

Figure 3. Frequency spectra obtained from temporal variation of transverse velocity at one location in the near wake. (a) Re_d=350 (b) Re_d=500 (c) Re_d=650. The dotted line in (a) is the spectra obtained by Bagchi and Balachandar using a different solver.

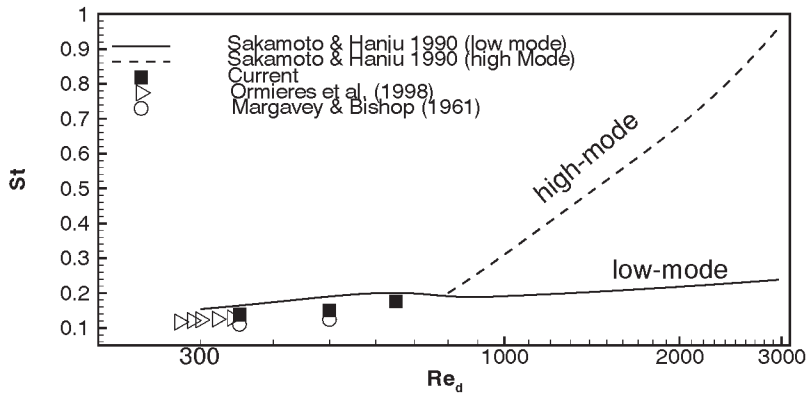

Figure 4. Variation of Strouhal number with Reynolds number.

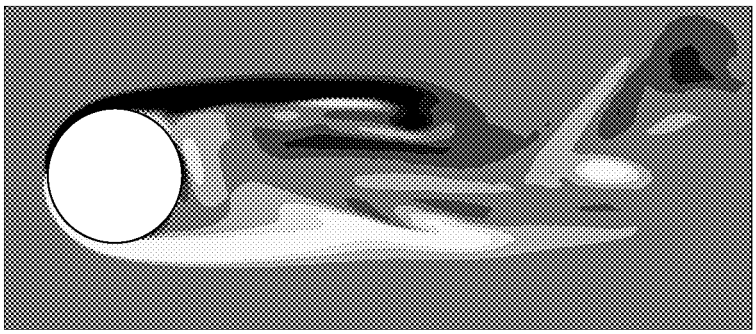

Figure 5. Contour plot of azimuthal vorticity at one time instant in the sphere wake at Re_d=650.

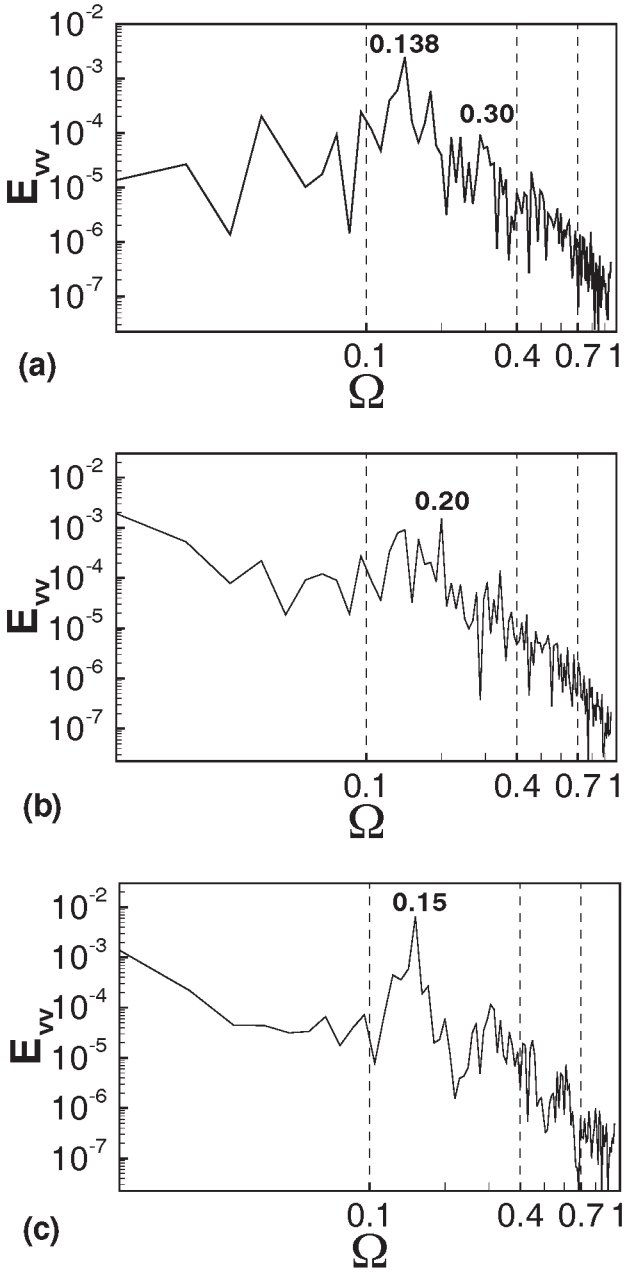

Figure 5. Power spectra obtained from temporal variation of transverse velocity at one location in forced sphere wake.(a) Ω_e=0.30 (b) Ω_e=0.20 (c) Ω_e=0.15.